KURENAI
Kyoto University Research Information Repository

KYOTO UNIVERSITY

Title	Dislocation nucleation in a thin Cu film from molecular dynamics simulations: Instability activation by thermal fluctuations
Author(s)	Umeno, Yoshitaka; Shimada, Takahiro; Kitamura, Takayuki
Citation	PHYSICAL REVIEW B (2010), 82(10)
Issue Date	2010
URL	http://hdl.handle.net/2433/148377
Right	© 2010 The American Physical Society
Type	Journal Article
Textversion	publisher

Kyoto University

Dislocation nucleation in a thin Cu film from molecular dynamics simulations: Instability activation by thermal fluctuations

Yoshitaka Umeno,[1,][*] Takahiro Shimada,[2] and Takayuki Kitamura[2]

[1]*Institute of Industrial Science, The University of Tokyo, 4-6-1, Komaba, Meguro-ku, Tokyo 153-8505, Japan*

[2]*Department of Mechanical Engineering and Science, Graduate School of Engineering, Kyoto University, Yoshida-hommachi, Sakyo-ku, Kyoto 606-8501, Japan*

To elucidate the mechanism responsible for structural instability at the atomic level, atomistic modeling simulation of tension in a Cu thin film containing a notch was performed using an embedded-atom method potential and dislocation nucleation was observed. Mechanical stability during tension was analyzed by solving the eigenvalue problem of the Hessian matrix taking into account all the degrees of freedom of the atoms in the system. Since an eigenvalue designates the curvature of the potential energy landscape in the direction of the corresponding eigenvector, which indicates a deformation mode, the system is unstable under vanishing temperature at the critical strain (ε_c) when any eigenvalue is zero or negative. At a strain smaller than ε_c where all the eigenvalues are positive, atomic fluctuations due to finite temperature may cause structural instability. We found that the path of activated instability (dislocation emission from the notch) could be written with a linear combination of the eigenvectors having small eigenvalues obtained under a corresponding external strain at zero temperature. The energy landscape has a much lower hill along the mixed-mode path than along any single-mode paths. In a molecular dynamics simulation under finite temperature, components of deformation modes having small eigenvalues fluctuate at low frequency, which dominate the activation of instability.

I. INTRODUCTION

The structural stability of materials subject to external load is one of the most fundamental mechanical properties and is important for understanding the strength of materials. Since solid materials consist of atoms in cohesion interacting with one another via electrons, it is essential to investigate structural stability at the atomistic level, i.e., how atomistic lattices collapse under load or strain. For example, dislocations, which are line defects dominating plasticity, usually nucleate from a defect when local crystal lattices collapse under shear stress. Cracks propagate owing to the rupture of interatomic bonding near the crack tip under tension. It is therefore important to find the mechanism responsible for mechanical instability in atomistic structures to gain a better understanding of why plastic deformation occurs.

Many atomistic modeling studies on the criteria for mechanical instability have been carried out thus far. The instability of crystals under load has been investigated by means of the soft mode of phonons.[1,2] Although this scheme can detect the onset of structural instability at the atomistic level in pristine crystals, such as dislocation nucleation in films without defects, it cannot easily be applied to disordered atomic structures where phonon dispersion is not defined. On the other hand, defining the instability parameter for each atom by applying the Born criterion[3] to the local elastic stiffness of each atom[4,5] has been suggested in an attempt to investigate the instability of disordered atomic structures. This criterion designates the mechanical instability of a perfect lattice subject to load and this has been used for discussing the instability of pristine crystals.[6–11] The physical meaning of the atomic-instability parameter is, however, not clear, and the scheme cannot accurately detect the structural-instability criterion.

To tackle the instability problem in nonuniform structures, we have proposed a scheme for evaluating the mechanical instability that can be applied to arbitrary structures and loading conditions.[12,13] The scheme solves the eigenvalue problem of the Hessian dynamical matrix taking into account all the degrees of freedom (DOFs) that atoms in a system possess, which enables the instability criterion and the deformation mode to be rigorously evaluated, i.e., the system is unstable when the minimum eigenvalue becomes zero and the corresponding eigenvector represents the instability mode. One can obtain valuable insights into the fundamental process of plasticity through this analysis, such as how atoms move at instability and the size of the region related to unstable deformation.[14] The scheme is difficult to apply to large-scale systems where the dimensions of the Hessian matrix ($\sim 3N \times 3N$, where N is the number of atoms in the system) are so large that the computation for solving the eigenvalue problem becomes too expensive. However, a modified way of efficiently solving the instability problem has been developed by reducing the degrees of freedom that need to be considered,[15,16] which paves the way for applying the scheme to instability problems with various types of systems to enable structural instability at the atomistic level to be better understood.

By means of this scheme, eigenvalues and corresponding eigenvectors in a system subject to external loading at vanishing temperature have been investigated and those at the onset of instability have been examined to discuss how they are related to concomitant deformation. The physical meaning of (positive) eigenvalues and eigenvectors, on the other hand, in a mechanically stable system has not yet been sufficiently discussed. In reality, unstable deformation can occur in such systems owing to atomic fluctuations under a finite temperature. It is therefore important to investigate how the eigenvalues and eigenvectors are related to the fluctuations

and how instability is activated under finite temperatures, i.e., it is necessary to clarify the path for deformation in the phase space that a system with thermal fluctuations follows. Although the optimal transition path has been investigated in many studies thus far by means of rather static analyses to obtain the saddle point on the energy surface, there has been little discussion on how the system actually traces a path on the energy surface under finite temperatures, which can be deviated from the optimal path, and the mechanism behind this. The suggested scheme for deformation-mode analysis enables us to elucidate the mechanism for structural transition by monitoring the contribution each mode makes to the transition.

In this study, we carried out atomistic simulation using a metal thin-film model that was subject to tension and investigated dislocation nucleation from a surface notch. Focus was placed on two areas: (a) the evolution of instability modes during tension under a vanishing temperature and their relation to unstable deformation at the critical strain (ε_c) and (b) the mechanism for the activation of instability due to thermal fluctuations that occurs at $\varepsilon < \varepsilon_c$ under a finite temperature. This paper is organized as follows. In Sec. II, we first review the formalism of mechanical-instability analysis, and then demonstrate the analysis of the thin-film model during tension under a zero temperature. In Sec. III, we discuss our molecular dynamics (MD) simulation under a finite and relatively low temperature at $\varepsilon < \varepsilon_c$ to examine how instability is caused by thermal fluctuations and discuss its relation to instability modes. Section IV is the conclusion.

II. MECHANICAL INSTABILITY OF ATOMISTIC SYSTEM IN TENSION

A. Criterion of mechanical instability

When a solid material is subject to increasing external strain or load, unstable deformation generally occurs at a certain point (the critical strain or load). Here, we present an overview of how to rigorously treat this problem at the atomistic level. Let us take the case of tensile load or strain as an example.

1. Tension under vanishing temperature

We will begin by considering tension under a temperature (T) of 0 K, where there are no thermal fluctuations of atom positions. While the strain or load (stress) is increasing, the atoms are always located in optimal positions. For strain-controlled tension, mechanical instability is evaluated under constant strain conditions at a given volume. To evaluate instability under load-controlled tension (constant load condition), the degrees of freedom of the volume (simulation cell matrix) and the atoms have to be taken into account. The energy landscape of a system under increasing external strain or load is schematically outlined in Fig. 1. Here, we present the derivation of equations for rigorously analyzing the mechanical instability of an atomistic system.

Degrees of freedom of system with/without periodic boundaries. Consider a system consisting of N atoms.
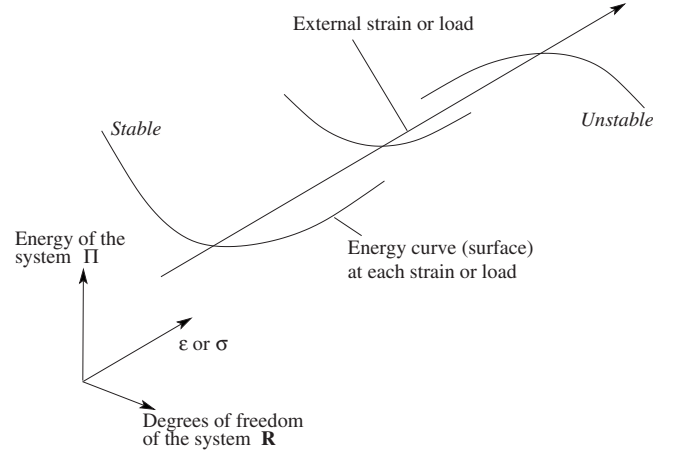

FIG. 1. Schematic of energy curves (surfaces) changing under increasing external strain or load.

First, let the system be free standing in a vacuum where no body force is exerted. The number of DOFs of the whole system, M, is $3N-6$; the DOFs of atoms ($3N$) subtracted by those for translation (3) and rotation (3) of the system. The potential energy of the system, U, is a function of a $3N-6$-dimensional vector, **R**,

$$U = U(\mathbf{R}). \qquad (1)$$

For the three-dimensional periodic boundary condition, the DOFs of the three vectors designating the cell,

$$\mathbf{a} = \begin{pmatrix} a_x \\ a_y \\ a_z \end{pmatrix}, \quad \mathbf{b} = \begin{pmatrix} b_x \\ b_y \\ b_z \end{pmatrix}, \quad \mathbf{c} = \begin{pmatrix} c_x \\ c_y \\ c_z \end{pmatrix}, \qquad (2)$$

are added, resulting in $M=3N-6+9=3N+3$. For example, we can construct a configuration vector (**R**) by fixing one atom on the origin of the coordinate, letting **c** be on the z axis and constraining **b** on the yz plane, i.e.,

$$\mathbf{R} \equiv (r_x^{(2)}, r_y^{(2)}, r_z^{(2)}, r_x^{(3)}, r_y^{(3)}, r_z^{(3)}, \dots,$$
$$r_x^{(N)}, r_y^{(N)}, r_z^{(N)}, a_x, a_y, a_z, b_y, b_z, c_z), \qquad (3)$$

where the superscripts indicate atom numbering.

Instability criterion and mode under constant load condition. Let the system be in an equilibrium state with vanishing kinetic energy (temperature $T=0$ K), i.e., the atoms are located at an optimum site and are in balance with the external load. According to the energy principle in the mechanics of elasticity, the total potential energy, Π, is the summation of the internal strain energy, U, and the potential energy of the external load, W ($\Pi = U + W$), since we are considering a system that has no body force.

For brevity, we will first consider an isolated body (no periodic boundary condition) in balance with the external force exerting on some surface atoms. The Taylor series expansion of Π with respect to the infinitesimal deformation, $\delta\mathbf{R}$, gives

$$\Pi(\mathbf{R} + \delta\mathbf{R}) = \Pi(\mathbf{R}) + \sum_{m=1}^{M} \frac{\partial\Pi}{\partial R_m} \delta R_m$$

$$+ \frac{1}{2}\sum_{m=1}^{M}\sum_{n=1}^{M} \frac{\partial^2\Pi}{\partial R_m\,\partial R_n}\delta R_m\delta R_n + \cdots$$

$$= \Pi(\mathbf{R}) + \sum_{m=1}^{M} \frac{\partial U}{\partial R_m}\delta R_m + \sum_{m=1}^{M} \frac{\partial W}{\partial R_m}\delta R_m$$

$$+ \frac{1}{2}\sum_{m=1}^{M}\sum_{n=1}^{M} \frac{\partial^2 U}{\partial R_m\,\partial R_n}\delta R_m\delta R_n + \cdots$$

$$+ \frac{1}{2}\sum_{m=1}^{M}\sum_{n=1}^{M} \frac{\partial^2 W}{\partial R_m\,\partial R_n}\delta R_m\delta R_n + \cdots, \quad (4)$$

where R_m represents the DOFs of atom α in the i direction, $R_m = r_i^{(\alpha)}$.

Here, the force on atom α in the i direction, F_m, is given by

$$F_m = -\frac{\partial U}{\partial R_m}. \quad (5)$$

Note that the right term is zero for atoms on which no external force is exerted. From the potential of external load, we get

$$\frac{\partial W}{\partial R_m} = -f_m, \quad (6)$$

where f_m is a force exerting on atom α in the i direction. Since the external force is constant,

$$\frac{\partial^2 W}{\partial R_m\,\partial R_n}\delta R_m\delta R_n = 0. \quad (7)$$

Considering the equilibrium condition, $F_m - f_m = 0$, and neglecting higher terms, we obtain

$$\delta\Pi \equiv \Pi(\mathbf{R} + \delta\mathbf{R}) - \Pi(\mathbf{R}) = \frac{\partial^2 U}{\partial R_m\,\partial R_n}\delta R_m\delta R_n. \quad (8)$$

The left-hand side of Eq. (8) represents the increase in system energy during the infinitesimal deformation of $\delta\mathbf{R}$. The negative value of $\delta\Pi$ indicates that the energy of the system can decrease under constant external load, i.e., the system is unstable. In contrast, the system is stable when $\delta\Pi$ is positive.

The case of the periodic boundary condition can be similarly considered. Here, the DOFs of the cell matrix (global strain) are included in $\mathbf{R}$ (and in $\delta\mathbf{R}$). The derivative of U with respect to global strain divided by the volume corresponds to the applied global stress, which cancels out with the derivative of W with respect to global strain. As a result, $\delta\Pi$ can be expressed in the same form as Eq. (8).

Introducing Hessian matrix $\mathbf{A}$, whose components are given by

$$A_{mn} = \frac{\partial^2 U}{\partial R_m\,\partial R_n}, \quad (9)$$

δI can be written in matrix form,

$$\delta I = \frac{1}{2}\delta\mathbf{R}^{\mathrm{T}}\mathbf{A}\,\delta\mathbf{R}, \quad (10)$$

where $^{\mathrm{T}}$ means transposition.

Now, solving the eigenvalue problem of matrix $\mathbf{A}$,

$$\mathbf{A}\mathbf{p}_i = \eta_i\mathbf{p}_i \quad (i = 1, 2, \ldots, M), \quad (11)$$

we get eigenvalues, η_i $(i = 1, 2, \ldots, M)$ $(\eta_1 < \eta_2 < \cdots < \eta_M)$, and eigenvectors, $\mathbf{p}_i$ $(i = 1, 2, \ldots, M)$. We let $\mathbf{p}_i$ be normalized. We then obtain

$$\mathbf{p}_i^{\mathrm{T}}\mathbf{A}\mathbf{p}_i = \eta_i\mathbf{p}_i^2 = \eta_i. \quad (12)$$

Since the eigenvectors are an orthogonal basis set (we can choose orthogonal vectors for degenerated eigenvectors), we can write infinitesimal deformation as

$$\delta\mathbf{R} = \sum_{i=1}^{M} \alpha_i\mathbf{p}_i. \quad (13)$$

Therefore, considering Eq. (10), the energy shift by $\delta\mathbf{R}$ becomes

$$\delta I = \frac{1}{2}\sum_{i=1}^{M} \alpha_i^2\eta_i. \quad (14)$$

This equation shows that η_i designates the curvature of the energy surface, $\delta I(\{\delta\mathbf{R}\})$, along $\mathbf{p}_i$. Thus, when $\eta_1 > 0$ (all the eigenvalues being positive) the system is stable; δI is positive with respect to arbitrary infinitesimal deformation. On the other hand, when η_1 is negative, δI can be negative with respect to $\delta\mathbf{R} = \mathbf{p}_1$, meaning that the system is unstable along $\mathbf{p}_1$, which may be called the unstable deformation mode.

Under constant strain condition. Under the condition of fixed boundaries or constant strain, the potential energy of external load is not considered and the DOFs of the cell matrix are not included in the infinitesimal deformation vector, $\delta\mathbf{R}$. The energy difference with respect to $\delta\mathbf{R}$ is therefore

$$\Pi(\mathbf{R} + \delta\mathbf{R}) = \Pi(\mathbf{R}) + \sum_{m=1}^{M} \frac{\partial U}{\partial R_m}\delta R_m$$

$$+ \frac{1}{2}\sum_{m=1}^{M}\sum_{n=1}^{M} \frac{\partial^2 U}{\partial R_m\,\partial R_n}\delta R_m\delta R_n + \cdots. \quad (15)$$

The equilibrium condition gives

$$\sum_{m=1}^{M} \frac{\partial U}{\partial R_m}\delta R_m = 0. \quad (16)$$

5.12 Å

19.8 Å

25.0 Å
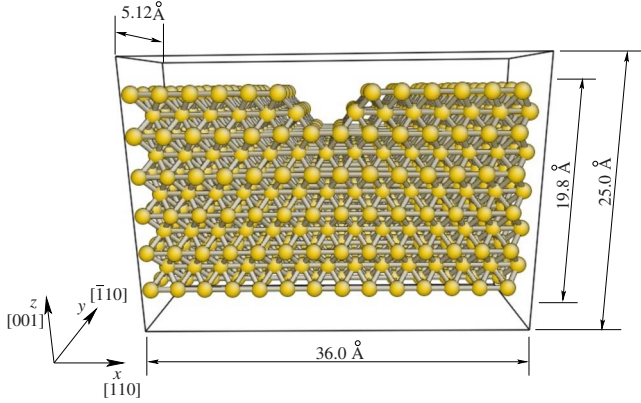
36.0 Å

z
[001]

y [$\bar{1}$10]

x
[110]

FIG. 2. (Color online) Simulation cell of Cu thin film with notch.

Neglecting higher terms, we obtain

$$\delta\Pi \equiv \Pi(\mathbf{R} + \delta\mathbf{R}) - \Pi(\mathbf{R}) = \frac{\partial^2 U}{\partial R_m \, \partial R_n} \delta R_m \delta R_n. \quad (17)$$

Equation (17) has a form identical with that of Eq. (8).

2. Tension under finite temperature

Next, we will consider tension under a finite temperature. While the system is subject to controlled and increasing external strain or load, the atoms move around the optimal positions because of thermal fluctuations. At each (fixed) strain or load, the system moves on the energy surface, $\Pi(\mathbf{R})$. While the oscillation of atom positions due to thermal fluctuations is small under a relatively low temperature, the amplitude of oscillation increases under an elevated temperature. To quantitatively evaluate the mechanical instability of a system under elevated temperatures, one must consider the profile of the free energy instead of the potential energy and take a statistical average of the system state. Thus, the instability criterion must be formulated on the basis of the change in the free energy against deformation. Under relatively low temperatures where the effect of thermal fluctuations is moderate, however, one may consider that the energy profile designating instability is close to that of the potential energy. Instability analysis based on the vanishing temperature,

which is much easier to analyze than that based on free energies, may give us useful insights into instability at relatively low temperatures.

B. Instability mode in tension

1. Simulation procedure

Figure 2 shows the simulation cell used in this study containing $N=302$ atoms with a size of $L_x \times L_y \times L_z = 36.0(\text{Å}) \times 5.12 \times 25.0$. Cu atoms were arranged with a lattice constant of $a=3.61$ Å and a notch was introduced on the surface. Boundaries were periodic only in the x and y directions to achieve a thin-film model. The generalized embedded atom method (GEAM) interatomic potential proposed by Zhou *et al.* was employed.[17]

The global strain, ε_{xx}, was increased stepwise and the atomic configuration was relaxed at each strain until the maximum force exerted on atoms becomes less than 10^{-8} eV/Å. This very stringent tolerance for relaxation was necessary to analyze the instability mode. The fast inertial relaxation engine [FIRE (Ref. 18)] algorithm introduced by Bitzek *et al.* was employed for efficient relaxation. During stretching and relaxation, L_y remained unchanged. The increment of the tensile strain, $\Delta\varepsilon_{xx}$, was 0.002 until $\varepsilon_{xx}=0.044$ and was then reduced to $\Delta\varepsilon_{xx}=0.0002$.

2. Change in eigenvalues during quasistatic tension

Figure 3 plots the change in tensile stress in the x direction, σ_{xx}, during tension. Snapshots of the atoms are also shown. The value of σ_{xx} at $\varepsilon_{xx}=0$ is nonzero because the GEAM potential slightly underestimates the equilibrium lattice constant of Cu and because a notch has been introduced on the surface. The sharp drop in tensile stress corresponds to the occurrence of unstable deformation, where a dislocation is emitted from the notch (toward the bottom right in the snapshot).

Figure 4 plots eigenvalues of the Hessian matrix as a function of tensile strain. We obtain 906 ($=M$) discrete eigenvalues at each strain. We draw curves based on the continuity of the eigenvalue for each mode confirmed by the form of the eigenvector, which will be demonstrated later. Here, we present the ten smallest eigenvalues, and they are denoted by mode 1, mode 2, …, based on the initial eigenvalues (at $\varepsilon_{xx}=0$). As seen in the figure, the order of eigen-

$\varepsilon_{xx} = 0.0440$

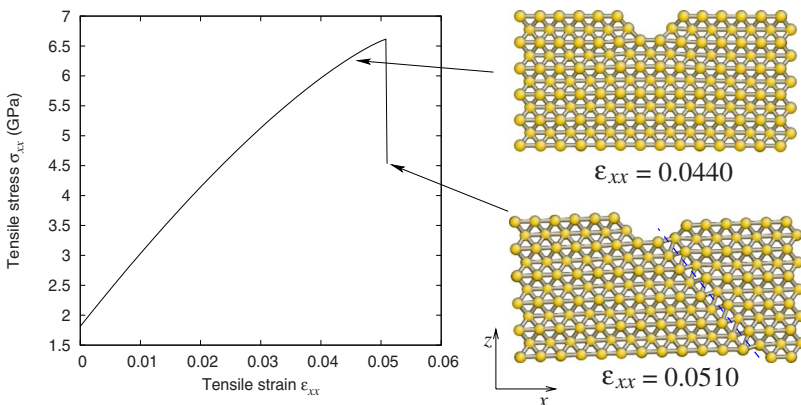$\varepsilon_{xx} = 0.0510$

z

x

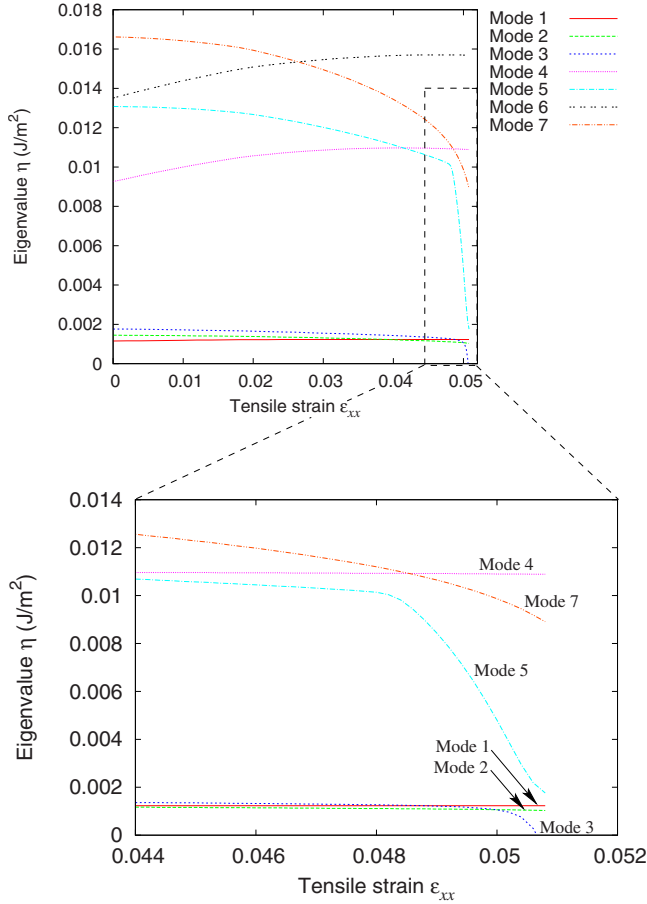FIG. 3. (Color online) Stress-strain curve and snapshots of atoms during tension.

FIG. 4. (Color online) Change in eigenvalues of Hessian matrix during tension. Bottom figure is magnification of top one.

values may change as strain grows. The eigenvalue of mode 3 becomes negative at $\varepsilon_{xx}=0.0508$, which corresponds to the instability of the system. The eigenvalues for modes 1 and 2 are small in the initial state and stay nearly unchanged during tension, which indicates that the initial magnitude of eigenvalues is not related to which mode becomes unstable.

3. Change in instability mode vectors during tension

Figure 5 shows the change in the instability mode vectors, **p**, at a strain of $\varepsilon_{xx} \geq 0.044$. The vector form of mode 1 indicates that it is a bending mode around the z axis, the form of which does not change much during tension. However, the vector distribution of mode 3 exhibits salient change. While large vectors are distributed over a large area at $\varepsilon_{xx}=0.0440$, the vectors become concentrated as the strain increases and only several atoms around the tip of the notch possess large magnitude right before instability occurs ($\varepsilon_{xx}=0.0508$). This indicates that dislocation nucleation is triggered by these unstable atoms around the notch.

The instability mode vectors in mode 3 have a mirror symmetry along the x axis. However, the instability occurring at $\varepsilon_{xx}=0.0508$ causes dislocation nucleation and propagation on the right of the notch, leaving the atom configuration on the left unchanged. The instability mode vector, **p**, indicates the direction of atom motion at the onset of un-

stable deformation and does not directly correspond to atom displacement during deformation (i.e., the relaxation process at $\varepsilon_{xx}=0.0508$). Here, the displacement becomes concentrated on the right side of the notch as deformation progresses, leading to dislocation nucleation and propagation.

When **p** meets Eq. (11), $-\mathbf{p}$ is also a solution to the eigenvalue problem. That is,

$$\mathbf{A}(-\mathbf{p}_i) = \eta_i(-\mathbf{p}_i) \quad (i = 1, 2, \dots, M). \quad (18)$$

This means that the reversed vectors (having an opposite sign) of those in Fig. 5 are also instability modes. The relationship between the sign of **p** and the direction of dislocation nucleation (propagation) is illustrated in Fig. 6. **p** and $-\mathbf{p}$ correspond to dislocations propagating in the bottom-right and bottom-left directions, respectively.

III. INSTABILITY PATH AT CRITICAL STRAIN UNDER RELATIVELY LOW TEMPERATURE

A. Unstable deformation due to thermal fluctuation

Now, let us consider material at strain where all the eigenvalues are positive. At a relatively low temperature, the system exhibits harmonic oscillation since the energy surface is approximately expressed by Eq. (14). At an elevated temperature, the amplitude of oscillation increases and it deviates from harmonic oscillation. The shape of the energy curve along a deformation mode, $\Pi(\alpha_i \mathbf{p}_i)$, can be of two types as schematically shown in Fig. 7. If the curvature of the energy curve is zero or positive anywhere ($\partial E/\partial \mathbf{R} \geq 0$), the energy always increases with increasing deformation. However, if the energy curve has a local maximum, i.e., a point where $\partial E/\partial \mathbf{R} < 0$, the material becomes unstable when the system goes beyond the energy peak. External conditions such as fluctuations caused by finite temperature may cause shifts in the configuration, **R**, resulting in the energy peak being transcended. That is, the system may become unstable with the activation of deformation modes that were originally stable. These modes can therefore be called "latent instability modes."

When kinetic energy is applied to the system where all the Hessian eigenvalues are positive, unstable deformation may occur owing to thermal fluctuations. That is, unstable deformation can occur under a finite temperature at strain smaller than the critical strain of deformation under vanishing temperature. For example, a dislocation nucleates from the notch at $\varepsilon_{xx}=0.0502$ in a molecular dynamics simulation with $T=20$ K. Although the change in the atomic configuration due to dislocation nucleation and propagation is similar to that in tensile deformation under 0 K, the mechanism for unstable deformation is different because the eigenvector of the minimum eigenvalue mode does not designate the deformation mode.

The eigenvalues of the Hessian matrix designate the shape of the energy surface at $\delta \mathbf{R}=0$ and do not determine that away from the optimal atomic configuration. When the system exceeds an energy hill and becomes unstable, its path is not necessarily in the direction of the mode
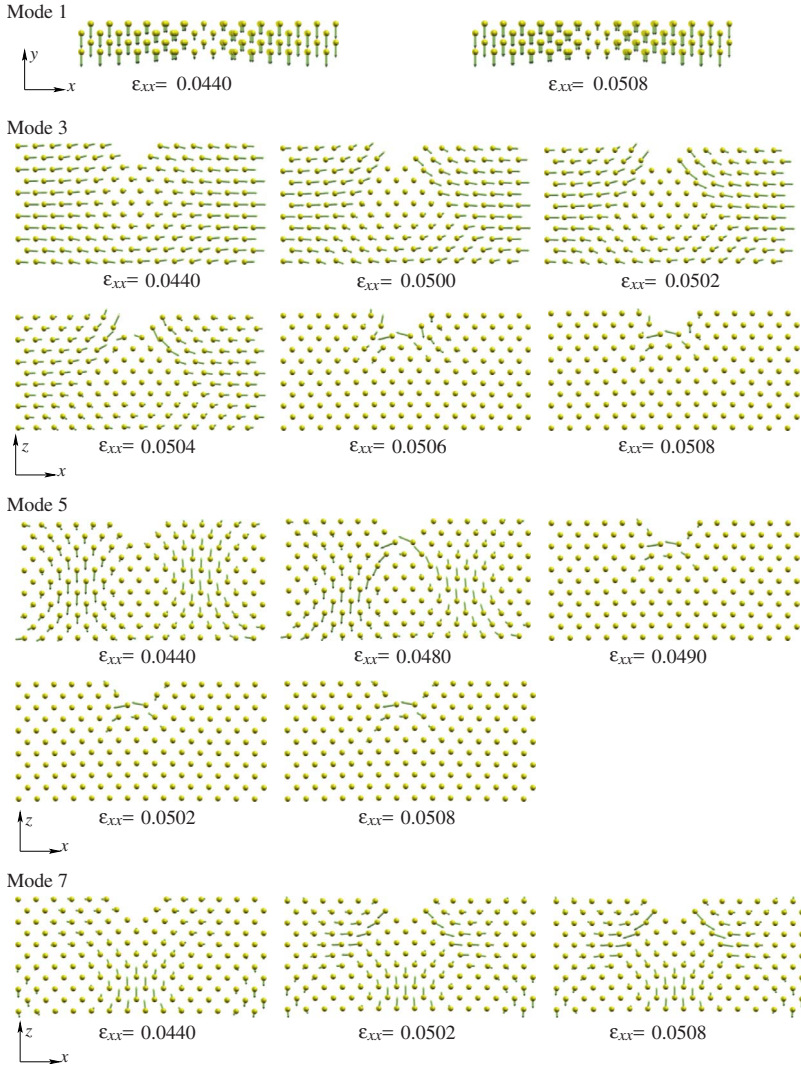
Mode 1

$\varepsilon_{xx}= 0.0440$ $\varepsilon_{xx}= 0.0508$

Mode 3

$\varepsilon_{xx}= 0.0440$ $\varepsilon_{xx}= 0.0500$ $\varepsilon_{xx}= 0.0502$

$\varepsilon_{xx}= 0.0504$ $\varepsilon_{xx}= 0.0506$ $\varepsilon_{xx}= 0.0508$

Mode 5

$\varepsilon_{xx}= 0.0440$ $\varepsilon_{xx}= 0.0480$ $\varepsilon_{xx}= 0.0490$

$\varepsilon_{xx}= 0.0502$ $\varepsilon_{xx}= 0.0508$

Mode 7

$\varepsilon_{xx}= 0.0440$ $\varepsilon_{xx}= 0.0502$ $\varepsilon_{xx}= 0.0508$

FIG. 5. (Color online) Change in eigenvectors (modes 1, 3, 5, and 7) of Hessian matrix during tension.

with the smallest eigenvalue. The curved surface $(f=-0.005x^4-0.005y^4+x^2+y^2-0.03x^2y^2)$ shown in Fig. 8 is a schematic of the energy landscape to illustrate this. While the landscape is nearly parabolic in the vicinity of the minimum-energy point, it deviates from this shape away from the point. As a result, a path along a mixed mode may have a lower energy hill (energy barrier) than that along a single mode. If, however, the energy surface is assumed to be smooth, one can speculate that the height of the energy hill will be low around the direction of deformation modes with

small eigenvalues. The figure shows a path between two modes for the sake of clarity, but one may have to consider mixing of more than two deformation modes, which can be expressed as a linear combination of the eigenvectors.

B. Instability path of notched component at critical strain

1. Simulation procedure

Using the relaxed configuration at $\varepsilon=0.0502$ obtained by the simulation of quasistatic tension as an initial state in the
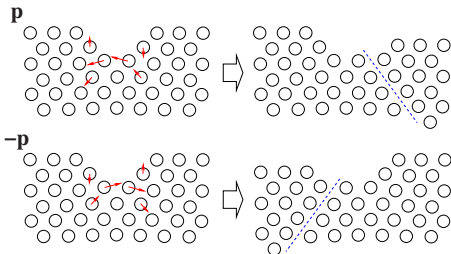

FIG. 6. (Color online) Schematics explaining relationship between instability mode (left) and direction of concomitant dislocation nucleation (right).
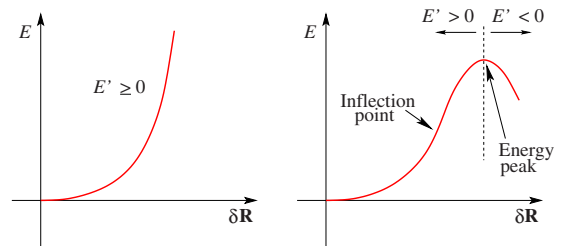

FIG. 7. (Color online) Schematics of energy curves with and without maximum energy. When curve is differentiable anywhere, maximum energy point is preceded by inflection point.
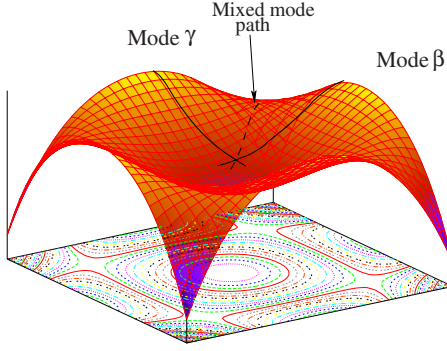
FIG. 8. (Color online) Schematic of energy hill along single-mode and mixed-mode paths.

previous section, MD simulation at the temperature $T=20$ K was performed. The velocity scaling method was used to control the temperature. Five different simulations (cases A–E) were carried out where the initial velocity was given by normal random numbers generated using different seed integers. The numerical integral of the equation of motion was solved by the velocity Verlet method using a time step, Δt, of 1.0 fs. The fluctuation behavior along with instabilities under the finite temperature was observed. Here, we observed the fluctuations under the condition of fixed strain for simplicity. The fluctuations under the fixed-stress condition are a little more complicated because one must take into account the change in potential due to external load accompanied by the change in volume during MD. The aim was to elucidate the mechanism behind the mechanical instability caused by thermal fluctuations by looking into the paths of the system state on the energy surface.

2. Simulation results

Figure 9 plots changes in the total energy of the system in the MD simulations of cases A–E. After a certain length of time, structural relaxation by dislocation nucleation occurs resulting in decrease in the total energy by about 4.0×10^{-20} J (0.25 eV). Owing to the difference in initial velocity, the number of steps until the dislocation nucleates differs.
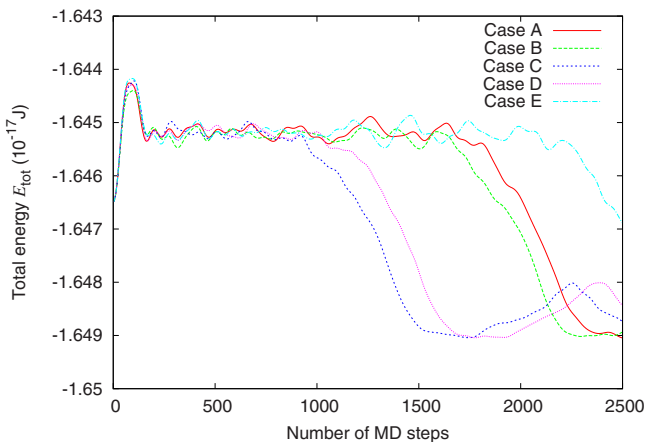

FIG. 9. (Color online) Change in total energy during MD calculations at $T=20$ K ($\varepsilon=0.0502$).
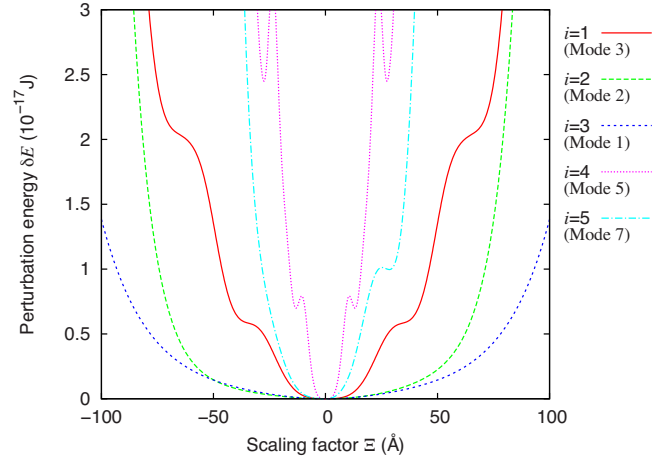

FIG. 10. (Color online) Perturbation energy as a function of atom displacement along deformation mode vector at $\varepsilon_{xx}=0.0502$.

Energy barrier in single mode. Now, we will consider the energy deviation, δE, from the energy of relaxed configuration at $\varepsilon_{xx}=0.0502$ ($T=0$ K) as a function of the infinitesimal displacement, $\delta\mathbf{R}$, along each deformation mode indicated by eigenvectors, i.e., we calculate

$$\delta E \equiv E(\mathbf{R}_0 + \delta\mathbf{R}) - E(\mathbf{R}_0), \tag{19}$$

where $\mathbf{R}_0$ is the relaxed configuration and

$$\delta\mathbf{R} = \Xi\mathbf{p}_i \quad (i=1,2,\ldots,M). \tag{20}$$

Here, we denote the modes by $i=1,2,\ldots$ from the one with the minimum eigenvalue. Figure 10 shows the energy deviation (perturbation) along modes 1, 2, 3, 5, and 7. The magnitude of the eigenvalues corresponds to the curvature of the energy curve at the origin [Eqs. (9) and (12)], which can be seen in the magnified plots.

In modes $1(i=3)$ and $2(i=2)$, the curvature around the origin is small, but the energy increases rapidly as $|\delta\mathbf{R}|$ increases. The energy curves for these modes are convex at least in the range of $\delta\mathbf{R}$ shown here, indicating that instability does not occur along these modes. The curve of mode $3(i=1)$ also increases monotonically with increasing $|\delta\mathbf{R}|$ although the curve has inflexion at $\Xi=\pm 22.6$ Å, exhibiting no local maximum.

However, the perturbation energy, δE, of mode $5(i=4)$ has inflexion at $\Xi=\pm 7.88$ Å and exhibits local maximum at $\Xi=\pm 10.6$ Å. The local maximum energy, $\delta E=8.05 \times 10^{-18}$ J (50.3 eV), is the energy barrier along mode 5 (single mode). The kinetic energy of the system is given by

$$E_{\text{kin}} = \frac{3}{2}Nk_{\text{B}}T, \tag{21}$$

where k_{B} is Boltzmann constant 1.38×10^{-23} J/K. In this system ($N=302$), the kinetic energy is $E_{\text{kin}}=1.25 \times 10^{-19}$ J (0.780 eV) at $T=20$ K, which is much lower than the energy barrier along mode 5. We can conclude that the thermal fluctuations at $T=20$ K are unlikely to cause the system to go beyond the energy barrier along mode 5.
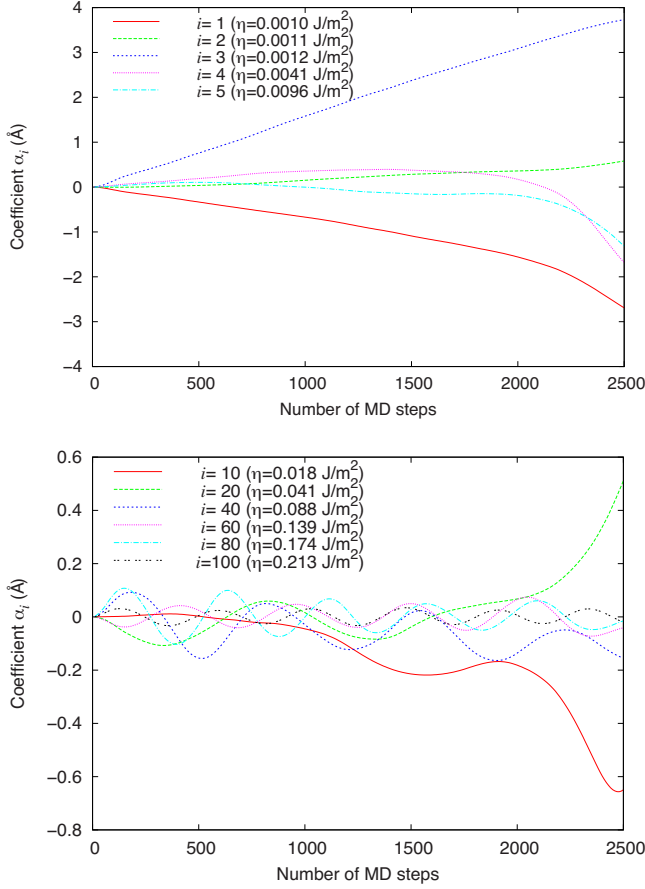
FIG. 11. (Color online) Change in α_i in Eq. (23) during MD calculation (case E).

Thermal fluctuations under finite temperature. As was explained in Sec. II A 1, the instability mode vectors (eigenvectors of the Hessian matrix at $T=0$ K), $\mathbf{p}_i$ $(i=1,2,\ldots,M)$, constitute the orthogonal system,

$$\mathbf{p}_i \cdot \mathbf{p}_j = \delta_{ij}, \qquad (22)$$

where δ_{ij} is the Chronecker delta, i.e., arbitrary vectors can be expressed by the linear combination of the mode vectors. Thus, an arbitrary vector of the atomic configuration, $\mathbf{R}$, can be expressed by

$$\mathbf{R} = \mathbf{R}_0 + \sum_{i=1}^{M} \alpha_i \mathbf{p}_i, \qquad (23)$$

where $\mathbf{R}_0$ is the equilibrium atomic configuration. The coefficients, α_i $(i=1,2,\ldots,M)$, are given by

$$\alpha_i = (\mathbf{R} - \mathbf{R}_0) \cdot \mathbf{p}_i. \qquad (24)$$

The change in the component of the modes in the displacement vector can be monitored by pursuing variations in α_i.

Figure 11 plots the evolution of the coefficients, α_i, in the MD simulation of case E. The coefficients of large i oscillate with relatively short cycles because the energy curves along the corresponding modes have large curvatures. The coefficients of small eigenvalues fluctuate moderately with relatively long cycles. The amplitude of the components of
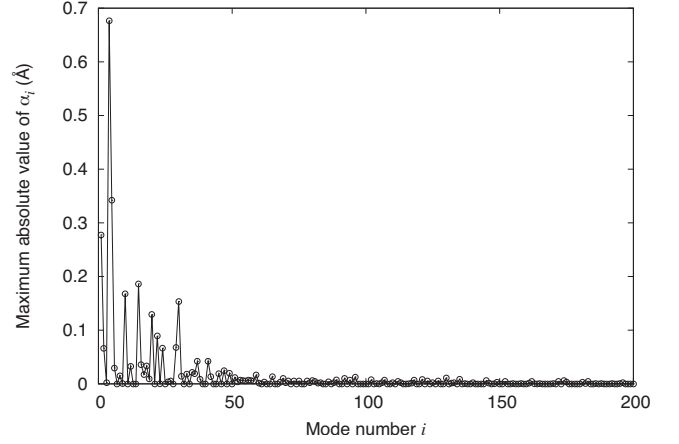

FIG. 12. Maximum absolute value of α_i during deformation along the minimum-energy path obtained by NEB analysis.

larger i tends to be smaller. The coefficients of small i exhibit salient change around 2000 steps corresponding to the structural change due to dislocation nucleation. The relationship between the amplitude and the magnitude of eigenvalues is not stringent, e.g., the amplitude of $i=80$ is much larger than that of $i=60$, which is because the initial velocity is given using random numbers.

C. Energy path

When unstable deformation is induced by kinetic energy, the system surmounts an energy hill with the height of activation energy. The optimal path for transition on the energy surface in the phase space is the minimum-energy path (MEP), which requires a minimum-energy cost for structural change. We obtained the MEP of dislocation nucleation at $\varepsilon=0.0502$ by using the nudged elastic band (NEB) method,[19,20] and then calculated the α_i components when the configuration changed along the MEP to nucleate a dislocation. The maximum absolute values of the components during the configuration transition along the MEP path are shown in Fig. 12. The results indicate that the components of the modes with large eigenvalues [mode numbers (i) larger than 50] are not invoked when the system goes along the MEP path. The MEP is constructed with the contribution made by many modes lower than $i=50$, meaning that modes with relatively small eigenvalues are relevant with unstable deformation (dislocation nucleation). Most salient among these modes are $i=4$ and 5, indicating that there may be a couple of modes that are dominant in the structural transition.

In MD simulation under a finite temperature, the system may go along a path that deviates from the MEP. It is therefore worth examining which modes are dominant in the unstable deformation of many modes activated along the MEP. Here, we examine if a mixed mode made up of a small number of modes presents a deformation path with a low-energy barrier.

Figure 13 shows the energy profiles along paths between modes 5($i=4$) and 7($i=5$). As shown in Fig. 13(a), the saddle points of the energy curved surface are in mixed mode paths.
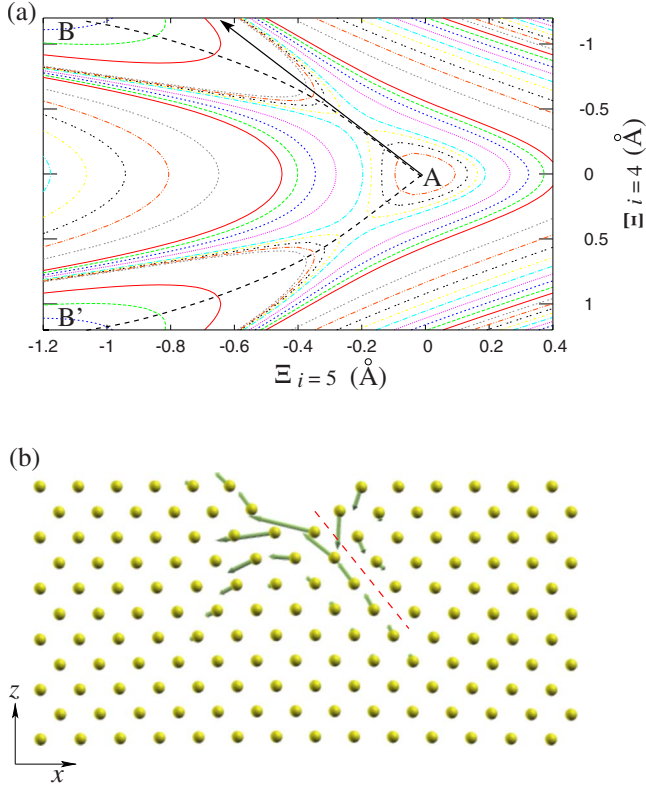
FIG. 13. (Color online) (a) Energy landscape of mixed mode of $i=4$ (mode 5) and 5 (mode 7). Contour plot of δE is shown. Local minimum points are indicated by A and B (B′) and minimum-energy paths of contour plot are indicated by dashed lines. (b) Deformation vectors in direction of solid arrow in (a).

The two paths, A→B and A→B′, correspond to the two directions of dislocation emission [to bottom-right and to bottom-left in Fig. 13(b), respectively]. The barrier height of the saddle points is substantially small, about 2.0×10^{-22} J (1.24×10^{-3} eV), which can be exceeded by the kinetic energy of $T=20$ K. The arrows in Fig. 13(b) present the mixed mode vectors along the solid line in Fig. 13(a), which indicate atom motion in the process of dislocation nucleation; atoms shear at the plane described by the dashed line.

In this section, we examine changes in the atomic configuration when instability induced by thermal fluctuations occurs under a finite temperature, i.e., we demonstrate how the atomic displacement vector of the M dimension moves on the energy curved surface in MD simulations under a finite temperature. As modes 5 and 7 ($i=4$ and 5, respectively) were shown to be related to dislocation nucleation in the previous section, we will now focus on the modes and discuss the changes in Fig. 14 in α_4 and α_5 in the MD simulations of cases A–D. The values of α_4 and α_5 change drastically when a dislocation is nucleated: The two coefficients exhibit substantial change when the total energy decreases from 1500 to 2000 steps in cases A and B and from 1000 to 1500 steps in cases C and D. The evolution of α_4 and α_5 indicates that in cases A, C, and D the system goes along the path of A→B in Fig. 13(b) while the path is A→B′ in case B.

As seen in Fig. 11, the fluctuations in the atomic configuration (displacement) consist of short-cycle components of
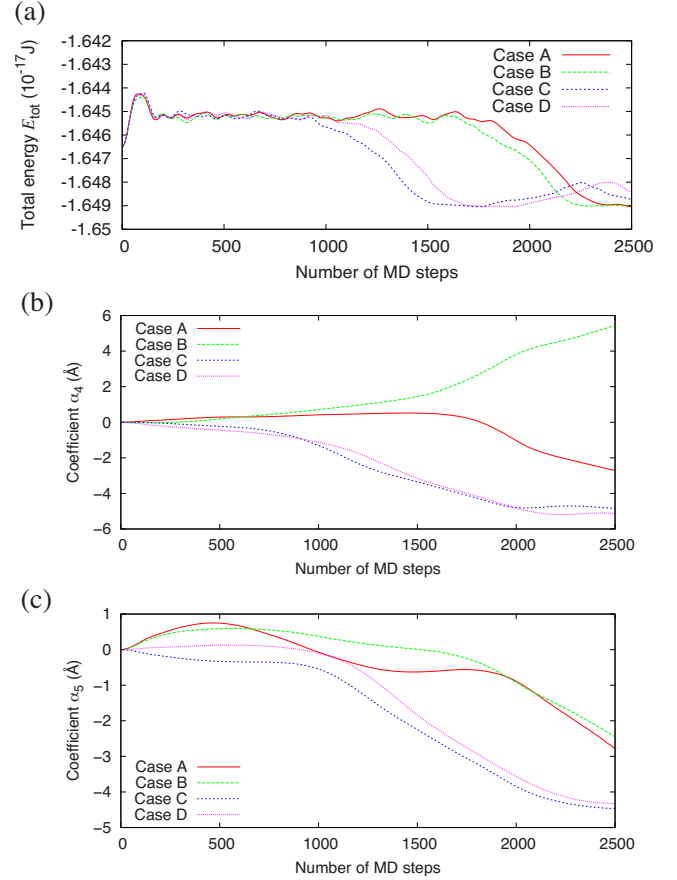

FIG. 14. (Color online) Change in (b) α_4 and (c) α_5 during MD (cases A–D). Change in E_{tot} is plotted again in (a).

modes with large eigenvalues and the long-cycle components of small eigenvalue modes. It should be reasonable to think that the former components indicate thermal vibration centered in the equilibrium atomic position. However, the latter components (long-cycle fluctuations) are related to changes in the atomic configuration due to unstable deformation. Here, we examine the fluctuations of modes with small eigenvalues in case A. As dislocation nucleation occurs at around 1750 steps in case A, we will now calculate the energy curve along the path indicated by the combination of modes $0 \leq i \leq M'$ at 1750 steps. That is,

$$\delta E = E(\mathbf{R}_0 + \delta\mathbf{R}') - E(\mathbf{R}_0), \qquad (25)$$

where

$$\delta\mathbf{R}' \equiv \xi \sum_{i=1}^{M'} \alpha_i \mathbf{p}_i. \qquad (26)$$

Here, ξ is a dimensionless coefficient. When $\xi=1.0$ and $M'=M$, $\mathbf{R}_0+\mathbf{R}'$ is identical to the atomic configuration at 1750 steps. Taking $M'<M$ means that mode components larger than M' are removed. By varying ξ, one can follow the atomic displacement along the path.

Figure 15 plots $\delta E(\xi)$. While no energy maximum is exhibited in the combination up to $i=4$ (modes 1, 2, 3, and 5), a maximum with a relatively low-energy height is present in
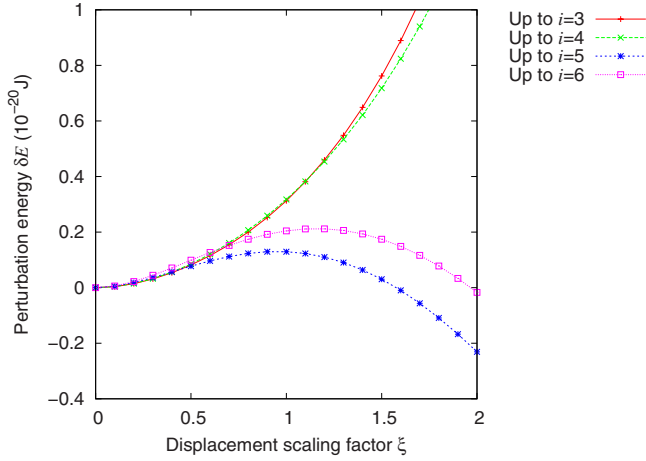
FIG. 15. (Color online) Energy profile along directions of mixed modes of low eigenvalues.
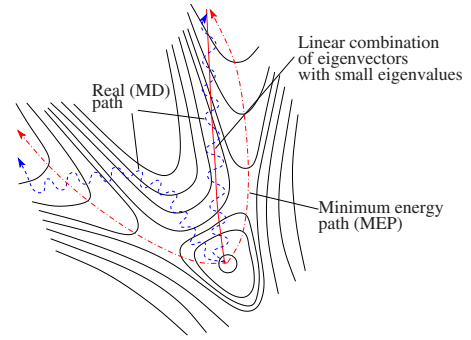

FIG. 16. (Color online) Schematic explaining paths to surmount energy hills. Dashed-dotted lines are lowest energy paths of dislocation nucleation. Winding dashed lines indicate trajectories of MD simulation at finite temperature. Solid line represents trajectory where fluctuations in higher modes have been removed.

the combination up to $i=5$. This corresponds to the fact that the mixed mode between $i=4$ and 5 is the path of dislocation nucleation that we saw in the previous section. The combination up to $i=6$ yields a higher energy maximum than that up to $i=5$, which is because the inclusion of mode $i=6$, which is not directly related to dislocation nucleation, shifts the displacement path away from the lowest energy path and moves it upward on the curved energy surface. The barrier height is much lower than the kinetic energy of the system at $T=20$ K. It should be noted here that the kinetic energy $(1.25 \times 10^{-19}$ J=0.780 eV) is that of the whole system and that the specific combination of α_i in the direction toward the energy hill should occur with relatively low probability.

The energy landscape around the mixed-mode paths is schematically illustrated in Fig. 16. Although the actual mode components (α_i) spread in M-dimensional space, here we have depicted the space by using the plane of the paper and the energy landscape by using contours. There can be plural paths of unstable deformation as indicated by the energy profile in Fig. 13. In MD simulations under finite temperatures, where fluctuations of all deformation modes are included, the system transcends an energy hill along a path with high-frequency fluctuations as indicated by the dashed curves. The solid curve, where the high-frequency fluctuations are removed, corresponds to the path in Fig. 15, for which a higher energy is required than that of the optimal instability path.

As plotted in Fig. 11, the amplitude of components of large i modes is small. While the MEP, which surmounts the lowest energy hill, requires contributions from modes with relatively large i, the components of large i modes are not likely to become sufficiently large through thermal fluctuations. In contrast, the combination of only several modes of small i can produce a path with a relatively low-energy hill. The system can easily meet such requirements during fluc-

tuations under a finite temperature as the amplitude of small i mode components may increase sufficiently, although the energy hill to go over is higher than that of MEP.

IV. CONCLUSION

To better understand the mechanism responsible for the occurrence of unstable deformation at the atomistic level, we analyzed atomistic level instability and examined the process of dislocation nucleation from a defect by means of atomistic modeling simulation using the empirical interatomic potential.

We discussed the physical meaning of the eigenvalues of the Hessian matrix with respect to the degrees of freedom in an atomistic system and found that positive eigenvalues correspond to the curvature of the potential-energy curve along deformation in the direction denoted by the eigenvector.

We performed simulations of the tensile deformation of a thin film containing a surface notch under a vanishing temperature. We demonstrated that the deformation mode that causes instability at the critical tensile strain is not related to the order of magnitude of eigenvalues in the initial state. We also found unstable atoms localized as the tension increased.

At the tensile strain that was slightly below the critical strain at 0 K, the potential-energy profile had a local maximum in the mixed-mode paths. While the optimal path for transition (MEP) was constructed with the contributions made by many modes with relatively low eigenvalues ($i \leq 50$), only a couple of them played an important role in creating an energy hill with relatively low activation energy. In MD simulation under a finite temperature at the tension, unstable deformation (dislocation nucleation) occurs when the components of the low i (≤ 6) modes meet the requirement to surmount the energy hill with heights taller than that of MEP, as the fluctuation amplitude of large i modes is modest.

*umeno@iis.u-tokyo.ac.jp

[1] K. J. Van Vliet, J. Li, T. Zhu, S. Yip, and S. Suresh, Phys. Rev. B **67**, 104105 (2003).

[2] S. Dmitriev, T. Kitamura, J. Li, Y. Umeno, K. Yashiro, and N. Yoshikawa, Acta Mater. **53**, 1215 (2005).

[3] M. Born and K. Huang, *Dynamical Theory of Crystal Lattices* (Oxford University Press, New York, 1954).

[4] T. Kitamura, K. Yashiro, and R. Ohtani, in *Mesoscopic Dynamics of Fracture: Computational Materials Design*, edited by H. Kitagawa, T. Aihara Jr., and Y. Kawazoe (Springer-Verlag, Berlin, 1998), pp. 120–130.

[5] K. Yashiro and Y. Tomita, J. Phys. IV **11**, 3 (2001).

[6] F. Milstein, Phys. Rev. B **3**, 1130 (1971).

[7] R. Hill and F. Milstein, Phys. Rev. B **15**, 3087 (1977).

[8] F. Milstein and R. Hill, J. Mech. Phys. Solids **25**, 457 (1977).

[9] F. Milstein and R. Hill, J. Mech. Phys. Solids **26**, 213 (1978).

[10] F. Milstein and B. Farber, Phys. Rev. Lett. **44**, 277 (1980).

[11] F. Milstein, J. Mater. Sci. **15**, 1071 (1980).

[12] T. Kitamura, Y. Umeno, and N. Tsuji, Comput. Mater. Sci. **29**, 499 (2004).

[13] T. Kitamura, Y. Umeno, and R. Fushino, Mater. Sci. Eng., A **379**, 229 (2004).

[14] Y. Umeno, T. Kitamura, and M. Tagawa, Mater. Sci. Eng., A **462**, 450 (2007).

[15] T. Shimada, S. Okawa, S. Minami, and T. Kitamura, Trans. Jpn. Soc. Mech. Eng., Ser. A **74**, 1328 (2008).

[16] T. Shimada, S. Okawa, S. Minami, and T. Kitamura, Mater. Sci. Eng., A **513-514**, 166 (2009).

[17] X. W. Zhou, R. A. Johnson, and H. N. G. Wadley, Phys. Rev. B **69**, 144113 (2004).

[18] E. Bitzek, P. Koskinen, F. Gähler, M. Moseler, and P. Gumbsch, Phys. Rev. Lett. **97**, 170201 (2006).

[19] G. Mills and H. Jónsson, Phys. Rev. Lett. **72**, 1124 (1994).

[20] *Classical and Quantum Dynamics in Condensed Phase Simulations*, edited by B. Berne, G. Ciccotti, and D. Coker (World Scientific, Singapore, 1998), pp. 385–404.